The Journal of Chemical Physics

RESEARCH ARTICLE | APRIL 29 2015

Force-extension curves for broken-rod macromolecules: Dramatic effects of different probing methods for two and three rods

A. V. Alexeev; D. V. Maltseva; V. A. Ivanov; L. I. Klushin; A. M. Skvortsov

Check for updates

J. Chem. Phys. 142, 164905 (2015)
https://doi.org/10.1063/1.4919295

View Online
Export Citation

17 April 2024 06:43:19

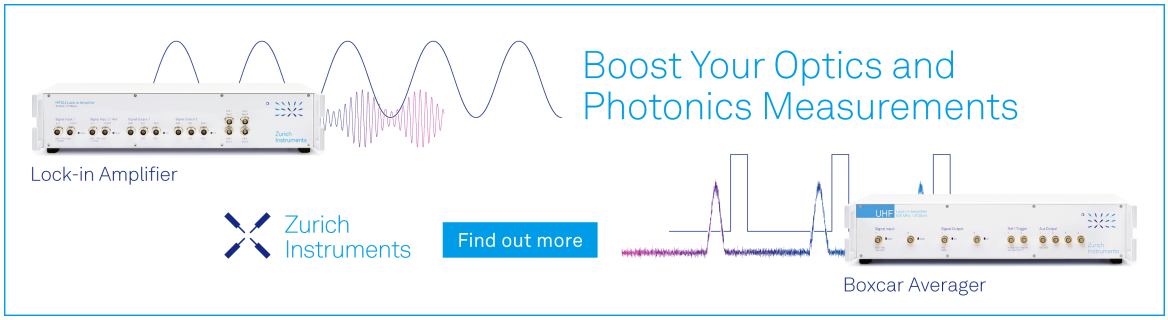

AIP Publishing

Force-extension curves for broken-rod macromolecules: Dramatic effects of different probing methods for two and three rods

A. V. Alexeev,[1] D. V. Maltseva,[1] V. A. Ivanov,[1,a)] L. I. Klushin,[2,b)] and A. M. Skvortsov[3,c)]
[1]*Faculty of Physics, Moscow State University, 119991 Moscow, Russia*
[2]*Department of Physics, American University of Beirut, P.O. Box 11-0236, Beirut 1107 2020, Lebanon*
[3]*Chemical-Pharmaceutical Academy, Prof. Popova 14, 197022 St. Petersburg, Russia*

(Received 11 December 2014; accepted 17 April 2015; published online 29 April 2015)

We study force-extension curves of a single semiflexible chain consisting of several rigid rods connected by flexible spacers. The atomic force microscopy and laser optical or magnetic tweezers apparatus stretching these rod-coil macromolecules are discussed. In addition, the stretching by external isotropic force is analyzed. The main attention is focused on computer simulation and analytical results. We demonstrate that the force-extension curves for rod-coil chains composed of two or three rods of equal length differ not only quantitatively but also qualitatively in different probe methods. These curves have an anomalous shape for a chain of two rods. End-to-end distributions of rod-coil chains are calculated by Monte Carlo method and compared with analytical equations. The influence of the spacer's length on the force-extension curves in different probe methods is analyzed. The results can be useful for interpreting experiments on the stretching of rod-coil block-copolymers. © *2015 AIP Publishing LLC.* [http://dx.doi.org/10.1063/1.4919295]

I. INTRODUCTION

Studies of elastic properties of amorphous polymers have long traditions.[1–3] The theory of rubber elasticity has connected the elastic response to entropic properties of long chains. Elastic response of an isolated polymer chain was first explored theoretically,[4–6] and this problem was initially considered as having a purely academic interest. However, the experimental situation has changed dramatically with the advent of new methods sensitive enough to probe individual macromolecules. Recent developments in mechanical experiments on single molecules provided a deeper understanding of intermolecular and intramolecular forces, thereby introducing crucial information about the thermodynamics and kinetics of biomolecular processes. One of the important single-molecule experiments concerns the stretching of the double-stranded and single-stranded DNA,[7–9] RNA,[10] proteins,[11] polysaccharides,[12] polyvinylamine,[9] and others. Single-molecule experimental methods are typically based on atomic force microscopy (AFM),[12,13] laser optical tweezers,[14,15] magnetic tweezers,[7,16] and polymer dynamics in an elongational flow.[17] A special interest in the behavior of individual semiflexible macromolecules has been triggered by the experiments with molecules of native double-stranded DNA, actin filaments, and microtubules. In recent years, statistical mechanics of semiflexible polymers has emerged as an active area of research. Theoretical examinations of semirigid macromolecules typically involve the model of a persistence chain to describe force-extension data on DNA,[18,19] mechanical properties of giant muscle protein titin,[20] polysaccharide dextran,[21] molecule of xantan,[22] and so on. The persistence length of the above objects is very high, especially that of actin and microtubule;[23,24] therefore, despite their large contour length, the number of Kuhn segments in these objects can be small.

In contrast to semiflexible polymers with persistent mechanism of rigidity, we concentrate on the deformation properties of chains whose flexibility is due to flexible spacers connecting relatively long rigid fragments (broken rod or rod-coil model). This flexibility mechanism is qualitatively different from that of a persistent chain. The latter requires considerable energy for a strong change in curvature but this can be distributed evenly along the chain contour. For the broken rod chain, changes in the curvature are localized but do not carry an energy penalty. The class of polymers described by the broken rod flexibility includes some synthetic copolymers consisting of rigid fragments connected by flexible spacers — see Fig. 1. The rod-coil molecules can consist of phenyl groups connected by ester linkages as the rod segment and a poly(propylene oxide) as the coil segment,[25] or high molecular weight helical polypeptides or poly(hexyl isocyanate) as rods connected to each other by either polystyrene or polybutadiene blocks as spacers.[26,27] The number of rod-coil blocks in most cases varies from one to three. Many of the syntheses of rod-coil copolymers as well as their interesting intriguing properties are discussed in books and reviews.[26,28] Apart from the wide range of different supramolecular structures in nanoscale dimensions, another unique characteristic is that rod segments can endow various functionalities such as photophysical and electrochemical properties to the supramolecular materials. The resulting rod-coil copolymers based on a polypeptide segment may serve as models providing insight into the ordering of complicated biological systems. Apart from this, close to the denaturation point of DNA double-stranded helix, the single-stranded parts develop flexible disordered sections with dramatically

a)Author to whom correspondence should be addressed. Electronic mail: ivanov@polly.phys.msu.ru
b)leo@aub.edu.lb
c)astarling@yandex.ru

17 April 2024 06:43:19

 © 2015 AIP Publishing LLC

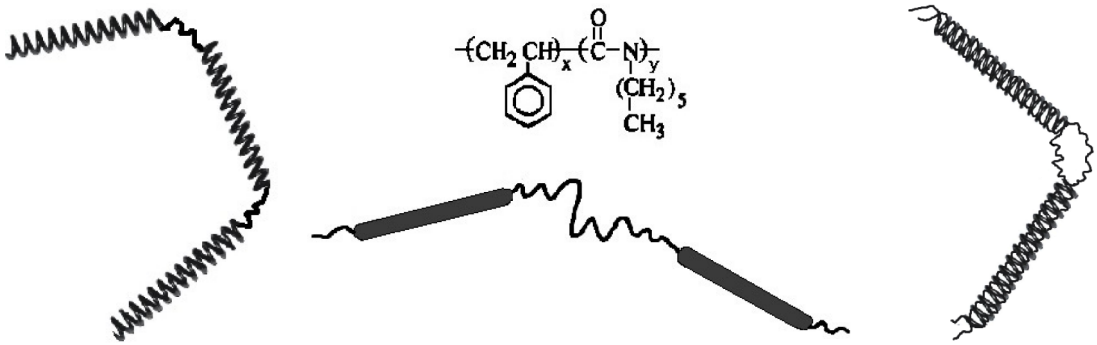

FIG. 1. Examples of the rod-coil macromolecules: helical polypeptide — flexible polybutadiene (a), rod-like poly(hexyl isocyanate) – flexible polystyrene (b), double-strand helix close to the denaturation point (c).

increased flexibility. These broken rod conformations are schematically represented in Fig. 1.

In this paper, we present Monte-Carlo (MC) simulations as well as rigorous analytical results for the elastic response of a chain composed of two or three jointed rods of equal length connected by much more flexible spacers. We show that the stress–strain curves of these chains obtained by different probing methods may be dramatically different. This is due to the purely entropic origin of elastic forces and we trace these differences to the underlying probability distributions. Because of their entropic nature, the forces concerned are quite small which may be of biological importance. It would be interesting to study also models with other mechanisms of chain flexibility, e.g., using semiflexible segments instead of rigid rods which should change slightly the elastic behaviour, but such a study is outside the scope of this paper.

The paper is organized as follows. In Sec. II, we elaborate on the various meanings of the phrase "force-extension curve." Section III introduces different probing methods and the relevant statistical distributions. Simulation method and the models used are described in Sec. IV. Results of the MC simulations for the force-extension curves corresponding to different probing methods are presented in Sec. V and compared to theoretical prediction. The background analytical theory is explained in Sec. VI where we also compare the predicted probability densities to the simulation results. Section VII analyses the influence of the spacer length on force-extension curves, while simulation results for the force-extension curves in the presence of strong steric hindrance effects are presented in Sec. VIII.

II. WHAT DOES "FORCE-EXTENSION CURVE" ACTUALLY MEAN?

"Perhaps the most elementary notion in polymer statistical mechanics is that to extend the ends of a long flexible molecule, a force must be applied."[18] The idea of a force-extension relationship for an individual macromolecule is extremely common and deceptively simple. There is a clear difference between applying a force directly to the chain ends and utilizing a force field that affects all monomers (as in a hydrodynamic flow). However, even if one concentrates on deformation by the ends, the picture is not as obvious as it may seem. It was understood early on that one can formulate two different ways of defining the force-extension curves. One method involves applying a fixed force and measuring the average of the fluctuating deformation; in the other, the deformation is fixed and the average of the fluctuation force is recorded. As noted by Flory, these two methods correspond to two different statistical ensembles — isotensional and isometric — analogous to Gibbs (NPT) and Helmholtz (NVT) ensembles in traditional statistical mechanics. It was shown that for a long flexible macromolecule with a Gaussian distribution of the end-to-end vector which is subject to extension along a fixed direction in space, the isometric and isotensional ensembles are equivalent in the thermodynamic limit of long chains, producing the same force-extension curve in this limit.[29–31] A series of recent publications explored the difference between the two statistical ensembles and their effects on the expected measurements of elastic properties of macromolecules deviating from Gaussian behavior, e.g., chains of rigid segments with and without excluded volume interactions.[30] Moreover, there was a general polemic on whether the ensemble equivalence theorem is applicable even to Gaussian chains.[32–36]

One of the main thrusts of the present paper is to stress that the subtlety of the question is not limited to the specification of the statistical ensemble. It is not enough to state, e.g., that the end-to-end distance is changed in a controlled way and the resulting force is measured, or, conversely, that the force is applied and the extension measured. Since both the force and the end-to-end separation are vectors, it matters whether we are specifying all three components, only one component (while the others are allowed to fluctuate), or the scalar magnitude. As shown below, various experimental methods of probing the elastic response turn out to be quite different in this respect, apart from the difference in the relevant ensembles.

To demonstrate the alarmingly confusing number of different settings, consider the Gibbs ensemble. The force may have a fixed magnitude and direction in space along Z-axis, $\vec{f} = f\vec{e}_z$ (see Subsection III A). The variable conjugate to the force is the z–component of the end-to-end vector as seen from the Boltzmann weight $\exp(\beta f z)$, where $\beta = 1/k_B T$, k_B is the Boltzmann constant, and T is the temperature. The measured response, however, can be taken either as $\langle z \rangle$, following the idea of conjugate variables, or as the scalar end-to-end distance, $\langle r \rangle$, following a more naive idea

17 April 2024 06:43:19

of what the chain extension means. If the chain end can only move along the Z-axis, there is no difference between z and $r = \sqrt{z^2 + x^2 + y^2}$. If the chain end is allowed to fluctuate freely in the (x, y) plane, the difference may be very large, as in the case of a strongly fluctuating, weakly deformed coil. With the first choice, the conjugate Helmholtz ensemble with fixed z is well defined (see Subsection III B) and the measured response is the average z-component of the force, $\langle f_z \rangle$. A setting with fixed z-coordinate with freely fluctuating (x, y)-coordinates is not obvious and may be difficult to realize experimentally. If the scalar distance is chosen as a controlled variable, the overall spherical symmetry guarantees that the average projection of the fluctuating vector force onto any fixed direction in space must vanish. The only meaningful non-zero response would be in the conjugate variable, i.e., the radial component of the force along the end-to-end vector. This, however, brings the notion of isotropic force and, possibly, a dramatically different force-extension curve, see Subsection III C. Part of the polemics in Refs. 33, 35, and 36 is due to the fact that certain important distinctions between conjugate and non-conjugate variables are ignored or misunderstood.

Although the difference between statistical ensembles has been discussed in some detail and their equivalence in the thermodynamic limit of infinitely long chains has been proven for particular classes of chain models,[29–31] much less attention was attracted to the fact that various experimental techniques of measuring the elastic response are, in fact, probing quite different statistical distributions. It turns out that this difference may be more dramatic than that related to the ensembles used.

Here, we do not pursue the comparison of different ensembles. Instead, we analyze two reasonably realistic and one more hypothetical experimental settings for probing the force-deformation curves. One of them naturally corresponds to the Helmholtz ensemble while the two others to the Gibbs ensemble.

III. EXPERIMENTAL METHODS AND RELEVANT STATISTICAL DISTRIBUTIONS

A. Stretching by magnetic levitation method

Magnetic levitation method was proposed in Ref. 37 and is based on the use of a superparamagnetic bead, see Figure 2. When placed in an external magnetic field B, the bead experiences a force $f = -\mu \nabla B$, where μ is the induced magnetic moment. In a relatively strong inhomogeneous field, the bead magnetization is close to saturation and therefore does not depend on the bead position. It was possible experimentally to produce the field configuration such that its gradient remains nearly constant within a reasonably large region of space (about 1 mm size). Thus the bead experiences a constant position-independent force, the magnitude of which can be varied within a broad range of values by appropriately placing the magnets with respect to the sample. Once the superparamagnetic bead is attached to the free end of the chain, it provides a stretching force. The set-up allows fluctuations of the end-to-end vector not only in the direction of the force applied but also in the lateral directions. The average z-coordinate of the chain end in this case is given by

$$\langle z \rangle_{magn} = \frac{\int_{-\infty}^{\infty} zP(z) \exp(\beta f z)\, dz}{\int_{-\infty}^{\infty} P(z) \exp(\beta f z)\, dz}, \tag{1}$$

where $P(z) = \int W(x, y, z)\, dxdy$ is the probability density for the z-coordinate and $W(x, y, z)$ is the probability density for the end-to-end chain vector $\vec{r} = (x, y, z)$ in the absence of any external forces.

It has been long known that stretching an ideal freely jointed chain by applying an end-force of fixed magnitude and direction is equivalent to the problem of orienting classical non-interacting spins by magnetic field, famously solved by Langevin.[4] The average extension normalized by the contour length as a function of force is given by

$$\frac{\langle z \rangle_{magn}}{NA} = \coth(\beta f A) - \frac{1}{\beta f A}, \tag{2}$$

where N is the number of rods and A is the length of one rod. Equation (2) is valid exactly for the magnetic levitation method irrespective of the number of rigid rods in the chain; this includes the case of $N = 1$.

In the low-strain limit, $z \ll NA$, the freely jointed chain exhibits linear elasticity

$$\frac{\langle z \rangle_{magn}}{NA} = \frac{\beta f}{3}. \tag{3}$$

B. Isometric AFM mode

Most of the experimental data on the elastic behavior of a single macromolecule were obtained by using AFM. In this method, one end of the chain is attached to a substrate, while the other undergoes a controlled motion along a straight line, which we denote the Z-axis. The average reaction force along the Z-direction, $\langle f \rangle$, is the measured response. According to the isothermal work theorem, this force is related to distribution density $W(x, y, z)$ for the end-to-end chain vector,

$$\beta \langle f_z \rangle_{AFM} = -\frac{\partial \ln W(0, 0, z)}{\partial z}. \tag{4}$$

For a long freely jointed chain consisting of $N \gg 1$ rods, the AFM force-extension curve $\langle f \rangle_{AFM}(z)$ is still approximately described by Langevin equation (2) with the change that the averaging applies to force rather than coordinate. This is guaranteed by the general theorem on ensemble equivalence in the $N \to \infty$ limit, corrections being of the order of N^{-1}.[38] Langevin equation is not applicable to AFM measurements with chains consisting of only a few rods, $N = 1, 2, 3$, as shown below. An ideal Gaussian chain would generate a linear force-elongation curve given by Eq. (3).

C. Stretching by isotropic force

In a typical experimental setting, the direction of an external force is specified by the macroscopic measuring device. One can also consider the effects of internal fields produced by interactions between various parts of the macromolecule, their orientation being determined by the chain conformation itself. This situation arises, for example, if the chain ends carry charges generating a Coulomb force. In this case, the stretching force would be caused by the interaction of

17 April 2024 06:43:19

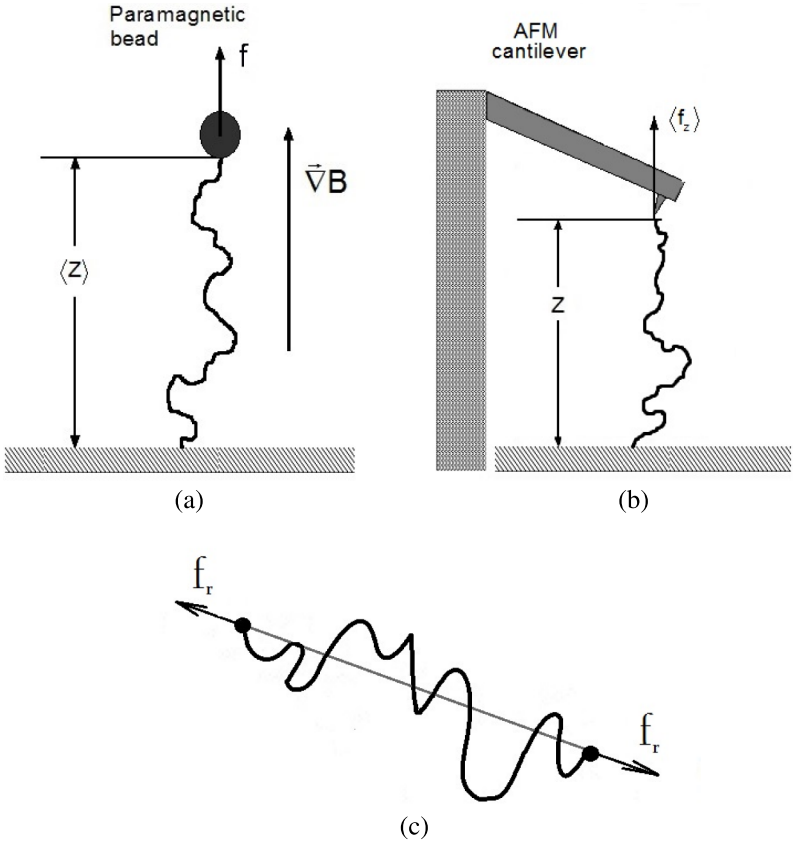

FIG. 2. Magnetic levitation method (a): measurement of the average height $\langle z \rangle$ as a function of external force f acting on a paramagnetic bead attached to the chain end; motion in (x, y) directions is not restricted by external forces, the magnetic force direction coincides with that of the magnetic field gradient. AFM method (b): average z-component of the force $\langle f_z \rangle$ is measured as a function of the height z of the chain at fixed values of (x, y). Isotropic force probe (c): measurement of the average scalar end-to-end distance $\langle r \rangle$ as a function of radial force f_r.

the chain ends between each other rather than with the external field. It is clear that, in this experiment, the interaction force between the ends would be a function of distance; its direction, however, is always radial, i.e., along the end-to-end vector, and fills the full solid angle isotropically as the macromolecule undergoes angular diffusion. A somewhat artificial situation in which the isotropic force is constant and its magnitude is an independent parameter has been the subject of considerable theoretical interest. This situation describes the behavior of the scalar end-to-end chain distance in a "correct" ensemble, with the scalar distance being precisely one of the conjugated parameters. The distribution function of the scalar distance between the ends of a polymer chain with consideration for all possible orientations of vector r in an isotropic situation is

$$W_{isotrop}(r) = 4\pi r^2 W(r). \tag{5}$$

The average scalar end-to-end distance is given by

$$\langle r \rangle_{isotrop} = \frac{\int_0^\infty r W_{isotrop}(r) \exp(\beta f_r r)\, dr}{\int_0^\infty W_{isotrop}(r) \exp(\beta f_r r)\, dr}. \tag{6}$$

In particular, for Gaussian chains,

$$W_{isotrop}(r) = 4\pi r^2 (2\pi N A^2)^{-3/2} \exp\left(-\frac{3r^2}{2NA^2}\right)$$

and the isotropic force-extension curve $\langle r \rangle_{isotrop}(f_r)$ has a closed-form expression in terms of error functions.[33] A much simpler expression[33] can be written as

$$\beta f_r \cong \frac{3\langle r \rangle}{NA^2} - \frac{2}{\langle r \rangle}. \tag{7}$$

This is strictly valid in the conjugate (isotensional) ensemble but can be utilized as a useful approximation in isometric ensemble with the error being of order N^{-1} and vanishing for long chains.[38]

D. Connection between different probing methods

Each of the methods discussed above is probing a particular distribution density, $W(0,0,z)$, $P(z)$, or $W_{isotrop}(r)$. However, these functions are clearly linked and can be expressed from each other. For an isolated macromolecule in free volume, the spatial probability density for the end-to-end chain vector, $W(x, y, z)$, possesses the overall spherical symmetry and thus actually depends only on scalar end-to-end distance r. For a displacement along a given line, e.g., Z-axis with $x = y = 0$, one has $r = |z|$ and thus $W(r)$ coincides with $W(0,0,z)$ for $z \geq 0$. The distribution density for a single coordinate, $P(z)$, can be written as

$$P(z) = \int W\left(\sqrt{x^2 + y^2 + z^2}\right) dxdy = 2\pi \int_{|z|}^{\infty} rW(r)dr. \tag{8}$$

This relation is easily inverted expressing the spatial density $W(r)$ as a function of scalar distance in terms of $P(z)$,

$$W(r) = \frac{1}{2\pi r}\left(\frac{dP}{dz}\right)_{|z|=r}, \tag{9}$$

which we utilize later on. Obviously, $W(0,0,z)$ is an even function of z and Eq. (9) is sufficient for defining it completely,

$$W(0,0,z) = \frac{1}{2\pi z}\frac{dP(z)}{dz}. \tag{10}$$

17 April 2024 06:43:19

Finally, the isotropic density $W_{isotrop}(r)$ is related to $W(r)$ by Eq. (5).

IV. MODEL AND SIMULATION METHOD

We have performed Monte Carlo computer simulations using both the conventional Metropolis algorithm[39] and Wang-Landau (WL) sampling.[40,41] In computer simulations, we have used the continuous model of freely jointed telescopic rods with average length $A = 1$ (this choice has fixed the units of length in our model). The maximal and the minimal lengths of a rod were equal to $A_{max} = 1.05$ and $A_{min} = 0.95$, respectively. There was no potential on the length of a rod.

Both the ideal chains and the chains with excluded volume have been studied by means of simulations. Results for ideal chains are presented in Sec. V. In this case, no interaction potential between rods was applied, i.e., the rods were assumed to be infinitely thin and phantom. Excluded volume effects can be roughly separated into short- and long-range effects. The former are dominated by interactions between two neighboring rods, which is equivalent to limiting the allowed range of angles between them. Long-range effects are universal and fall under scaling description. However, for chains consisting of a few rigid segments that we concentrate on, short-range effects are the most important as far as the qualitative features of the force-extension curves are concerned. By simulating both the ideal freely jointed model and the model with large excluded volume, we obtain lower and upper estimates of the possible range of excluded volume effects. Details of the model parameters for the chain with excluded volume are given in Sec. VIII.

One end of the chain was anchored to the origin of coordinates $(x, y, z) = (0, 0, 0)$. In the Metropolis MC simulations, the force of strength f was applied to another end. This force was directed along the Z-axis for magnetic levitation method and for AFM mode, while it was applied along the direction of the end-to-end vector in the case of stretching by isotropic force. Metropolis algorithm allows to calculate the average z-coordinate of the chain end, $\langle z \rangle$, or the average scalar distance between the chain ends, $\langle r \rangle$, and is suitable only for simulation of isotensional ensemble. Our main emphasis, however, was on simulations based on the WL method[40,41] which allows a direct evaluation of the distribution density $W(x, y, z)$, and the average force is determined according to Eq. (4). WL method can be used for both isotensional and isometric ensembles. We have compared the results for isotensional ensemble obtained by both methods in order to make sure that they coincide with each other. However, the statistics in WL simulations is much better, and therefore we show below only the results obtained by WL sampling. In WL simulations, we have performed 10^9 attempted moves per each of at least 27 iterations for given value of WL refinement factor γ, starting from initial value $\gamma_0 = e$ and ending with final value $\gamma_{26} \approx 1.000\,000\,01$. After each iteration i with given refinement factor γ_i, we have checked the flatness of the energy histogram, i.e., whether the average height was larger than 80% from the maximal height. If this flatness criterion was fulfilled, we have modified the refinement factor as $\gamma_{i+1} = \sqrt{\gamma_i}$. If this criterion was not fulfilled, we have made additional 10^9 attempted moves with the same refinement factor γ_i (the maximal total number of iterations was equal to 37).

The algorithm of conformation evolution was as follows: we have chosen a junction point between two successive rods randomly, applied random displacements dx, dy, dz along coordinate axes uniformly distributed in the interval $[-0.01, 0.01]$ and accepted it with probability p according to WL rules, $p = min\,[1, g(E_{old})/g(E_{new})]$, where $g(E)$ is the density of states with energy E and the indices *old* and *new* denote the conformations before and after the trial move, respectively. Because for ideal chains the only energy term is due to the external force, i.e., $E = -fz$ for magnetic levitation and AFM methods, where z is the z-coordinate of the chain end, and $E = -fr$ for isotropic force stretching, where r is the scalar distance between the chain ends, the density of states depends on the corresponding coordinate, $g(z)$ or $g(r)$, respectively. An important restriction for AFM probing mode is that the chain end can be displaced only along Z-axis, while in magnetic levitation method and in isotropic stretching method, any direction for chain end displacement is allowed. As was already mentioned above, in the isometric ensemble, the average force is determined according to Eq. (4), where $g(z)$ is used in place of $W(0, 0, z)$, while the average z-coordinate of the chain end (or the average scalar distance between the chain ends) in the isotensional ensemble is determined by the formula (compare with Eq. (1))

$$\langle z(f) \rangle = \frac{\sum_z z g(z) \exp(fz)}{\sum_z g(z) \exp(fz)}. \tag{11}$$

V. FORCE-EXTENSION CURVES FOR IDEAL ROD-COIL CHAINS

The force-extension curves corresponding to different measurement methods are presented in Figures 3–5 for ideal chains of $N = 10$, 3, 2 freely jointed telescopic rods without excluded volume. The rules of changing the length of telescopic rods provide large but finite elongational stiffness in a single rod but do not affect free rotation in all internal angles. The overall effect is equivalent to adding a small flexible spacer to strictly rigid rods in the analytical theory presented in Sec. VI. In theoretical calculation, each spacer was considered as a Gaussian coil with rms size $a = A/10$. We have also studied analytically the effect of the length of spacers for ideal chains, and we present these results in Sec. VII.

MC data for the chain of $N = 10$ rods simulating magnetic levitation and AFM measurements coincide within the statistical error and are very well described by Langevin equation (2), see Fig. 3. This is to be expected on the general grounds discussed in Sec. III. The deformation curve for an isotropic force is adequately described by Eq. (7) apart from the finite extensibility effects at large strains. The difference between the isotropic force-extension curve and the two others is in the repulsive (negative force) region at small end-to-end distances. This region corresponds to distances smaller than the equilibrium coil size ($R/NA \sim N^{-1/2} \simeq 0.32$ for $N = 10$) and is associated with a loop-like conformation. For asymptotically long chains, the repulsion region vanishes as $N^{-1/2}$, and then all three curves become identical. It is clear that as

17 April 2024 06:43:19

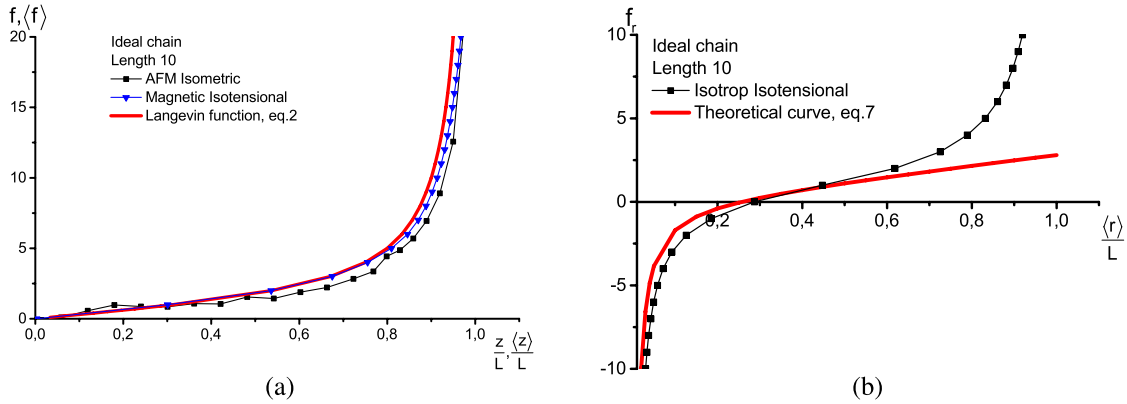

FIG. 3. Force-extension curves corresponding to AFM and magnetic levitation methods (a) and stretching by isotropic force (b). Symbols show the results of MC calculations, solid lines — analytical theory. The number of rods $N = 10$.

far as one compares the force extension curve for the magnetic levitation and AFM methods, N=10 is already asymptotically large, but for comparison to the isotropic force probe, N=10 is still quite far from the asymptotic limit.

Elastic properties of the chain consisting of three rods are displayed in Fig. 4 together with the predictions of the exact analytical theory presented in Sec. VI. As mentioned earlier (Sec. III), the curve describing the magnetic levitation method remains the same and is given by the Langevin equation irrespective of the number of rods in the chain. The isotropic curve develops a larger repulsive region in accordance with the $N^{-1/2} \simeq 0.58$ estimate. The change in the AFM curve is more specific. Theoretical curve shows that for strains $z/NA \lesssim 0.3$, the force is strictly zero; in the range $0.35 \lesssim z/NA \lesssim 0.65$, it develops a plateau value of $\frac{3kT}{2A}$; and only at larger strains, the force increases sharply. Simulation data support the theory well for each of the probing methods.

The most unusual elastic behavior is demonstrated by chains consisting of two rods connected by a small spacer, see Fig. 5. Again, simulations and theory agree very well for all three probing methods. The AFM curve develops a sharp maximum at small end separations, on the order of the equilibrium spacer size. Beyond that, the force is mostly a decreasing function of distance until the rods are nearly aligned and the

17 April 2024 06:43:19

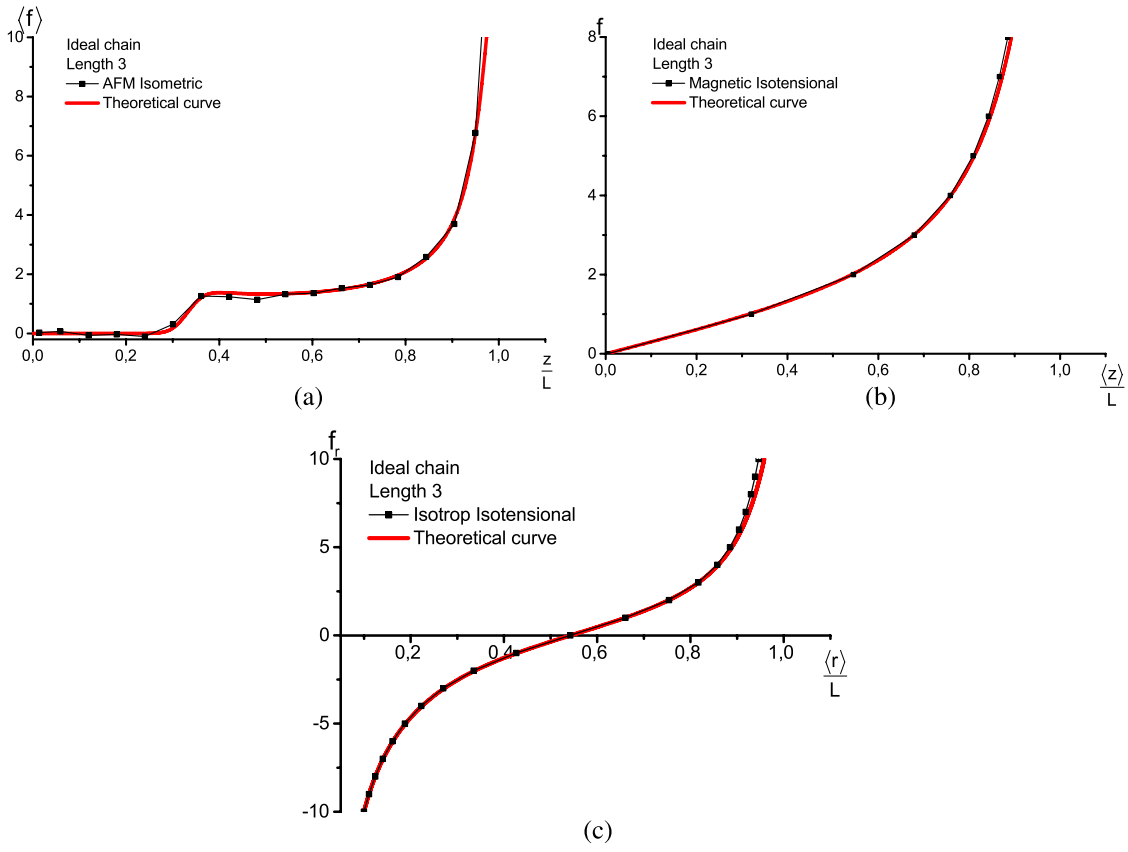

FIG. 4. Force-extension curves corresponding to AFM method (a), magnetic levitation method (b), and stretching by isotropic force (c). Symbols are the MC results, solid lines — analytical theory. The number of rods $N = 3$.

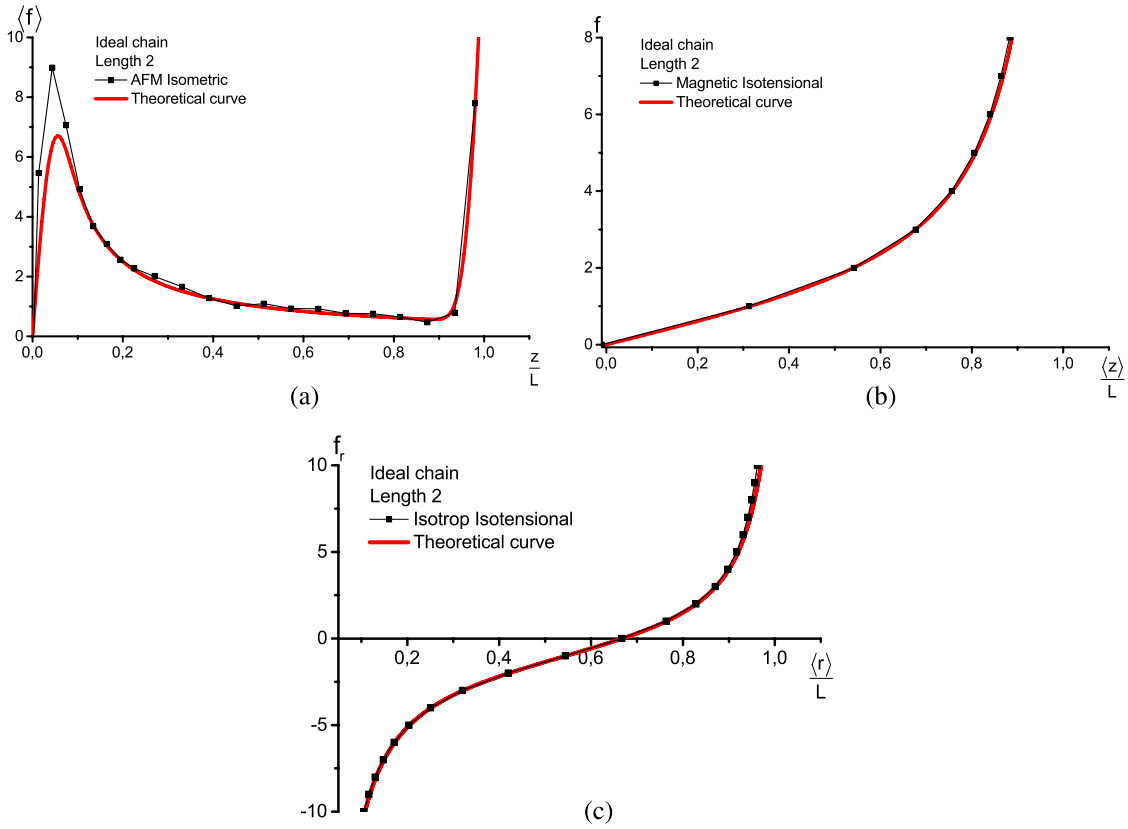

FIG. 5. Force-extension curves corresponding to AFM method (a), magnetic levitation method (b), and stretching by isotropic force (c). Symbols represent MC calculations, solid lines — analytical theory. The number of rods $N = 2$.

force is produced by the spacer deformation. It is clear from the overall view of the Fig. 5 that the force-extension curve is dramatically different illustrating the main message of this paper: the idea of the force-extension curve is not necessarily obvious and specifying the details of the probing method may be of crucial importance.

VI. ANALYTICAL THEORY FOR IDEAL ROD-COIL CHAINS

To analyze the force–extension curves for a chain composed of N rigid rods of equal length joined by $(N-1)$ flexible spacers, we need the different distribution densities introduced in Sec. III. From a practical point of view, $P(z)$ provides the most convenient starting point. The end-to-end chain vector is defined as the sum

$$\vec{r} = \sum_{i=1}^{2N-1} \vec{u}_i, \tag{12}$$

where $\vec{u}_i$ is the end-to-end vector of the i-th chain element (rod or spacer). Similarly, z is the sum of z-components of $\vec{u}_i$ vectors. Each of these is a random variable characterized by its distribution density. A single rod[42] is described by the density

$$P_{rod}(z,1) = \begin{cases} \dfrac{1}{2A} & |z| \le A \\ 0 & |z| \ge A \end{cases}, \tag{13}$$

where the second argument refers to the number of connected elements (rods or spacers). A single flexible spacer is described by

$$P_{sp}(z,1) = \sqrt{\frac{2}{3\pi a^2}} \exp\left(-\frac{3z^2}{2a^2}\right), \tag{14}$$

where a is the rms end-to-end distance of the spacer. For ideal chains, the distribution density for the total end-to-end z is clearly independent of the order of summation in Eq. (12) since each term represents an independent random variable. This means that the terms representing rigid rods can be grouped together to describe a freely jointed chain of N rigid rods, while the spacers are grouped to give a Gaussian chain of total rms size of $a\sqrt{N-1}$. The total probability density for the spacer group is thus

$$P_{sp}(z,N-1) = \sqrt{\frac{2}{3\pi(N-1)a^2}} \exp\left(-\frac{3z^2}{2(N-1)a^2}\right). \tag{15}$$

For the freely jointed rod group, the following recursion equation is valid:[6]

$$P_{rod}(z,k) = \int P_{rod}(z-z',k-1)P_{rod}(z',1)dz', \tag{16}$$

where $P_{rod}(z,k)$ is the relevant distribution density for the chain of k rods.

17 April 2024 06:43:19

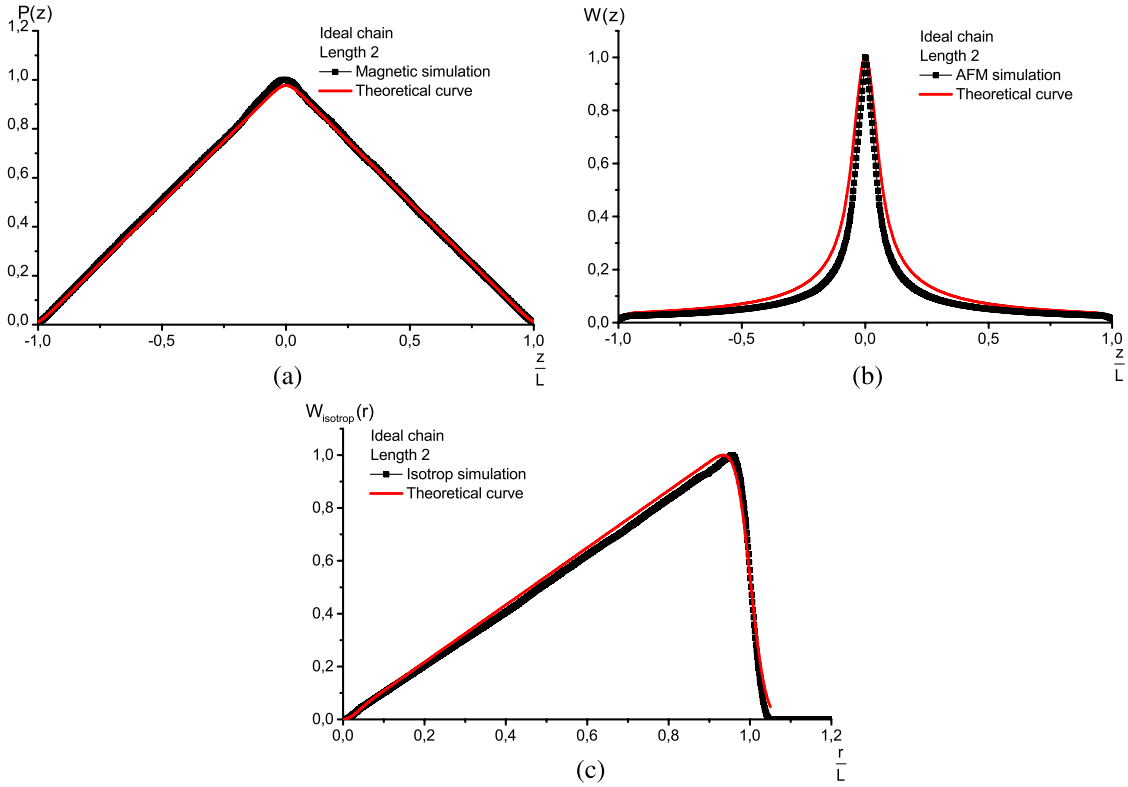

FIG. 6. Distribution of the end position for two rods with one spacer in magnetic mode $P(z,2)$ (a), in AFM mode $W(z,2)$ (b), and in isotropic mode $W_{isotrop}(r,2)$ (c). Solid lines — analytical theory, symbols — MC calculations for ideal chains.

For $N = 2$ and $N = 3$ rods, one obtains, respectively,

$$P_{rod}(z,2) = \begin{cases} (2A)^{-1}\left(1 - \dfrac{|z|}{2A}\right) & 0 \le |z| \le 2A \\ 0 & |z| \ge 2A \end{cases}, \quad (17)$$

$$P_{rod}(z,3) = \begin{cases} (8A)^{-1}\left(3 - \left(\dfrac{|z|}{A}\right)^2\right) & |z| \le A \\ (16A)^{-1}\left(3 - \dfrac{|z|}{A}\right)^2 & 1 \le |z| \le 3A. \\ 0 & |z| > 3A. \end{cases} \quad (18)$$

The final result (adding spacers to rods) is given by the convolution

$$P(z,N) = \int P_{rod}(z - z', N) P_{sp}(z', N-1) dz'. \quad (19)$$

The analytical result for two rods with one spacer has the following form:

$$P(z,2) = \frac{a}{4A^2}\sqrt{\frac{\pi}{6}} \exp\left(-\frac{3(2A+z)^2}{2a^2}\right) \times \left[1 + \exp\left(-\frac{12Az}{a^2}\right) - 2\exp\left(-\frac{6(A+z)^2}{a^2}\right)\right] + \frac{1}{8A^2}\left[(z-2A)\, erf\left(\frac{z-2A}{a\sqrt{2/3}}\right) - 2z\, erf\left(\frac{z}{a\sqrt{2/3}}\right) + (z+2A)\, erf\left(\frac{z+2A}{a\sqrt{2/3}}\right)\right], \quad (20)$$

where $erf(z)$ is the error function.

The resulting distribution $P(z,3)$ for three rods with two spacers is also expressed in terms of error functions but is too cumbersome to write out explicitly. The two remaining distribution densities, $W(0,0,z,N)$ and $W_{isotrop}(r,N)$, are obtained via Eqs. (10) and (5). Figures 6 and 7 demonstrate that the analytical theory predictions for various probability densities are very well supported by the MC simulations. The force-extension curves for different probing methods are calculated according to Eqs. (1), (4), and (6) and are shown earlier in Figures 4 and 5.

VII. INFLUENCE OF SPACER LENGTH ON FORCE-EXTENSION CURVES

The existing class of rod-coil block-copolymers includes macromolecules with a wide range of the relative size of the rod and the coil blocks. We have demonstrated above that a macromolecule consisting of two rods connected by a relatively small coil-like spacer of the rms a size 10 times smaller than the rod length A displays very unorthodox force-extension curves related to three different probing methods. It is clear, however, that once the coil-like spacer is taken large enough so that it dominates the overall size of the macromolecule, the anomalies in elastic behavior should disappear. In this section, we present the changes in the force-extension curves for a two-rod macromolecule with a systematic increase in the size of the spacer, $a/A = 0.1,\ 0.2,\ 0.5,\ 1$. Since the analytical theory is exact for ideal chains, we present only the theoretical curves. In all cases, the spacer is described by an ideal gaussian chain, and the range of chain extensions is limited to values close to the double rod length. It is assumed that finite extensibility of the spacer will show up at larger extensions. In the case

17 April 2024 06:43:19

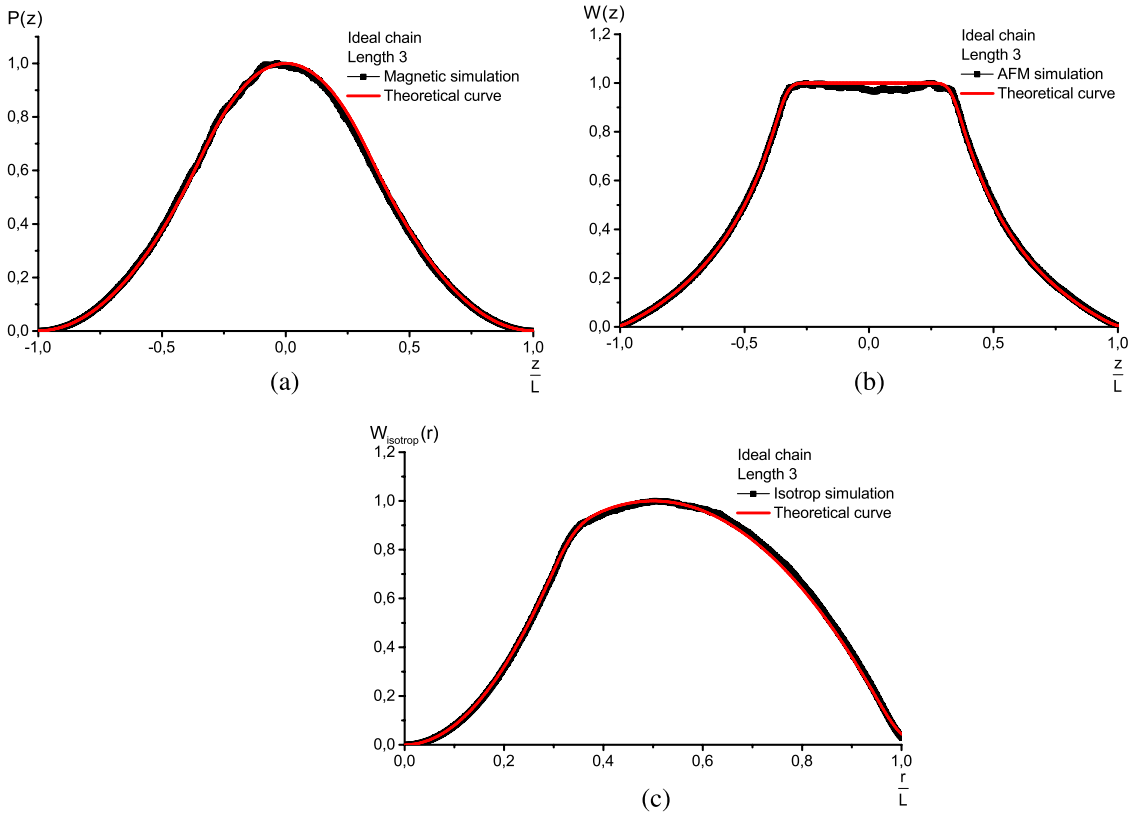

FIG. 7. Distribution of the end position for three rods with two spacers in magnetic mode $P(z,3)$ (a), in AFM mode $W(z,3)$ (b), and in isotropic mode $W_{isotrop}(r,3)$ (c). Solid lines — analytical theory, symbols — MC calculations for ideal chains.

17 April 2024 06:43:19

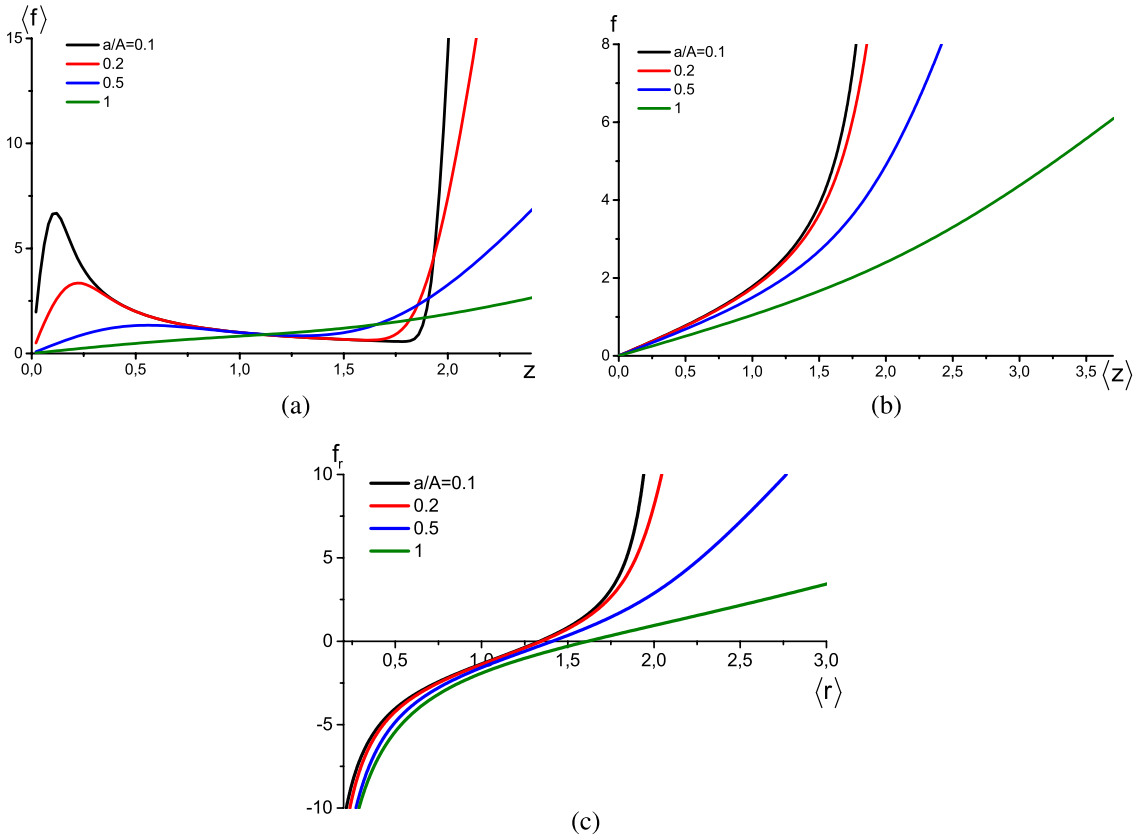

FIG. 8. Force-extension curves corresponding to AFM method (a), magnetic levitation method (b), and stretching by isotropic force (c) for macromolecules consisting from two rods with one spacer of different lengths. The length of spacer is $a/A = 0.1,\ 0.2,\ 0.5,\ 1$.

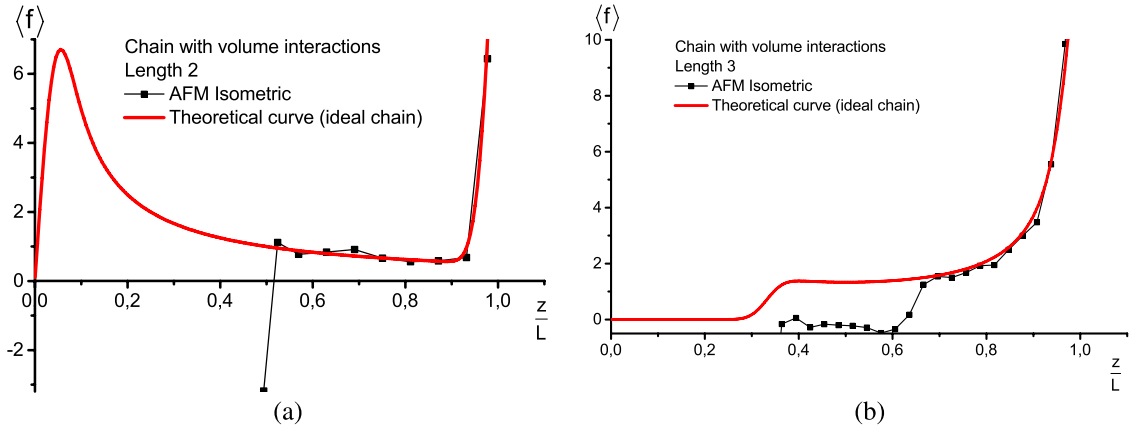

FIG. 9. Force-extension curves in AFM method for macromolecules consisting from $N = 2$ rods (a) and $N = 3$ rods (b). Symbols are the results of calculations by MC method with volume interactions; solid lines — theory for ideal coil-rod macromolecules.

of magnetic levitation and isotropic force curves, Figs. 8(b) and 8(c), increasing spacer length mostly softens the elastic response at larger extensions while the small-extension part of the curves changes only little. The AFM curves, Fig. 8(a), are strongly non-monotonic for shorter spacers but this effect gradually decreases and disappears completely when the rms spacer size is equal to the rod length.

VIII. STERIC HINDRANCE EFFECTS

In the standard polymer parlance, the phrase "excluded volume effects" implies the effects of interaction between monomers that are far from each other along the chain contour and lead to non-trivial scaling behavior. In this language, interaction of close neighbors along the chain can be incorporated in the definition of renormalized repeat units. Excluded volume effects in semiflexible chains have been studied in some detail (see Ref. 43 and references therein). In particular, it was shown that for moderately long persistent chains with a small d/l_p ratio where d is the thickness and l_p the persistence length, ideal Kratky-Porod behavior is observed. Nearly ideal behavior of moderately long chains consisting of strongly asymmetric rod-like repeat units (irrespective of the flexibility mechanism) is well understood since the dimensionless second virial coefficient for rods is small ($\sim d/A$). Thus, conventionally understood excluded volume effects in coil-rod macromolecules with very few rods cannot be strong. However, this does not preclude some short-range steric hindrance effects which are due to the geometric details of mutual attachment at the rod-coil-rod hinge and due to finite rod thickness. The former sets the minimum angle between the neighboring rods while the latter defines the minimum end-to-end distance. To estimate the maximum range of these effects, we have performed MC simulations with the impenetrable spheres of the radius 0.475 at both ends of each rod. This roughly corresponds to the rod thickness being equal to its length and means that the minimum end-to-end distance was equal to the minimal rod length A_{min}, and the minimum angle between adjacent rods was about $\pi/3$. Force-extension curves for magnetic levitation probing are practically unchanged in comparison to the ideal case for both $N = 2$ and $N = 3$ and hence are not shown here. The AFM curve for two rods is truncated at the minimum distance $z = A_{min}$ but the remaining part of the curve is unchanged, see Fig. 9(a). For three rods, the curve is also restricted to the range $z \geq A_{min}$ but qualitatively its shape with a near-zero range and a plateau remains the same, see Fig. 9(b). The main effect on the isotropic probe curves can be described as a quasi-affine compression along the r axis since the minimum distance has increased from 0 to A_{min} as shown in Fig. 10.

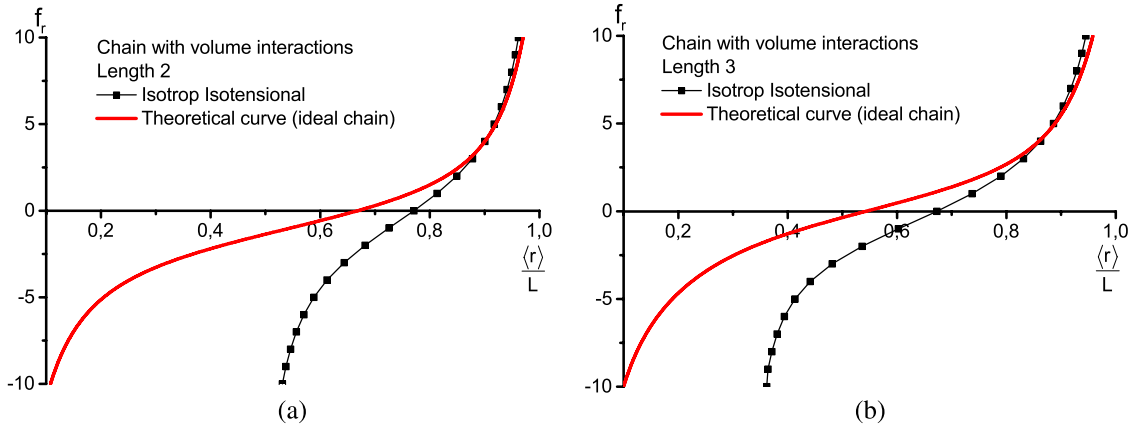

FIG. 10. Force-extension curves at stretching by isotropic force for macromolecules consisting from $N = 2$ rods (a) and $N = 3$ rods (b). Symbols correspond to calculations by MC method with volume interactions; solid lines — theory for ideal coil-rod macromolecules.

17 April 2024 06:43:19

IX. CONCLUSION

One of the main thrusts of the present paper is to stress that the notion of the force-extension relation for an individual macromolecule may be subtle. Different experimental methods (AFM, magnetic levitation, etc.) probe different statistical distributions and the resultant force-extension curves may turn out to be not just quantitatively but qualitatively different. We demonstrate this for strongly inhomogeneous block-copolymer chains composed of two or three long rigid rods connected via smaller coil-like spacers. The elastic response in question is of entropic nature and the corresponding forces are quite small.

ACKNOWLEDGMENTS

Financial support from RFBR (Grant Nos. 12-03-01137-a, 09-03-91344-NNIO-a, and 13-03-91331-NNIO-a) and DFG (Grant No. 436 RUS 113/863/02) is highly appreciated.

[1]W. Kuhn, Kolloid-Z. **68**, 2 (1942).
[2]W. Kuhn and F. Grun, Kolloid-Z. **101**, 248 (1942).
[3]R. G. Treloar, *Physics of Rubber Elasticity* (Clarendon, Oxford, 1975).
[4]M. V. Volkenshtein, "The configurational statistics of polymeric chains," J. Polym. Sci. **29**, 441 (1958).
[5]P. J. Flory, *Statistical Mechanics of Chain Molecules* (Hanser Publishing, Munich, 1989).
[6]A. Grosberg and A. Khokhlov, *Statistical Physics of Macromolecules* (American Institute of Physics, 2002).
[7]S. B. Smith, L. Finzi, and C. Bustamante, Science **258**, 1122 (1992).
[8]Y. Seol, G. M. Skinner, and K. Visscher, Phys. Rev. Lett. **93**, 118102 (2004).
[9]T. Hugel, M. Rief, M. Seitz, H. E. Gaub, and R. R. Net, Phys. Rev. Lett. **94**, 048301 (2005).
[10]J. Liphardt, B. Onoa, S. B. Smith, I. Tinico, Jr., and C. Bustamante, Science **292**, 733 (2001).
[11]M. Grandbois, M. Beyer, M. Rief, H. Clausen-Schaumann, and H. E. Gaub, Science **283**, 1727 (1999).
[12]M. Rief, M. Gautel, F. Oesterhelt, J. M. Fernandez, and H. E. Gaub, Science **276**, 1109 (1997).
[13]T. Hugel and M. Seitz, Macromol. Rapid Commun. **22**, 989 (2001).
[14]J. R. Moffitt, Y. R. Chemla, S. B. Smith, and C. Bustamante, Annu. Rev. Biochem. **77**, 205 (2008).
[15]A. Ashkin, Proc. Nat. Acad. Sci. U. S. A. **94**, 4853 (1997).
[16]C. Gosse and V. Croquette, Biophys. J. **82**, 3314 (2002).
[17]T. T. Perkins, D. E. Smith, and S. Chu, Science **5321**, 2016 (1997).
[18]J. F. Marko and E. D. Sigga, Macromolecules **28**, 8759 (1995).
[19]R. Winkler, J. Chem. Phys. **118**, 2919 (2003).
[20]M. Rief, F. Oesterhelt, B. Heymann, and H. E. Gaub, Science **5304**, 1295 (1997).
[21]M. Rief, J. M. Fernandez, and H. E. Gaub, Phys. Rev. Lett. **81**, 4764 (1998).
[22]H. Li, M. Rief, F. Westerhelt, and H. E. Gaub, Appl. Phys. A: Mater. Sci. Process. **68**, 407 (1999).
[23]A. Ott, M. Magnasco, A. Simon, and A. Libchaber, Phys. Rev. E **48**, R1642 (1993).
[24]F. Gittes, B. Mickey, J. Nennleton *et al.*, J. Cell Biol. **120**, 923 (1993).
[25]M. Lee, B.-K. Cho, M.-K. Oh, and W.-C. Zin, Macromolecules **34**, 1987 (2001).
[26]B. Gallot, Prog. Polym. Sci. **21**, 1035 (1996).
[27]M. Lee, B. K. Cho, and W. C. Zin, Chem. Rev. **101**, 3869 (2001).
[28]K. Loos and S. Munoz-Guerra, *Supramolecular Polymers Chapter 7: Microstructure and Crystallization of Rigid-Coil Comblike Polymers and Block Copolymer* (Marcel Dekker, New York, 2000).
[29]J. H. Weiner, *Statistical Mechanics of Elasticity* (Dover Publication, Inc., New York, 2002).
[30]R. G. Winkler, Soft Matter **6**, 6183 (2010).
[31]F. Manca, S. Giordano, P. L. Palla, and F. Cleri, Physica A **395**, 154 (2014).
[32]M. Susen, M. Sega, and C. Holm, Phys. Rev. E **79**, 051118 (2009).
[33]V. A. Ivanov, L. I. Klushin, and A. M. Skvortsov, Polym. Sci., Ser. A **54**, 602 (2012).
[34]R. M. Neumann, Biophys. J. **85**, 3418 (2003).
[35]R. M. Neumann, J. Chem. Phys. **138**, 157101 (2013).
[36]F. Manca, S. Giordano, P. L. Palla, R. Zucca, and F. Clery, J. Chem. Phys. **138**, 157101 (2013).
[37]F. Assi, R. Jenks, J. Yang, C. Love, and M. Prentiss, J. Appl. Phys. **92**, 5584 (2002).
[38]J. T. Titantah, C. Pierleoni, and J.-P. Ryckaert, Phys. Rev. E **60**, 7010 (1999).
[39]D. Frenkel and B. Smit, *Understanding Molecular Simulation: From Algorithms to Applications* (Academic Press, San Diego, 2002).
[40]F. Wang and D. P. Landau, Phys. Rev. Lett. **86**, 2050 (2001).
[41]F. Wang and D. P. Landau, Phys. Rev. E **64**, 056101 (2001).
[42]S. Sinha and J. Samuel, Phys. Rev. E **71**, 021104 (2005).
[43]H. P. Hsu and K. Binder, J. Chem. Phys. **36**, 024901 (2012).

17 April 2024 06:43:19